Earthline Journal of Chemical Sciences
E-ISSN: 2581-9003; CODEN: EJCSB4
Volume 13, Number 3, August 2026, Pages 245-257
https://doi.org/10.34198/ejcs.13326.19.245257

Study of the protection of aluminum in hydrochloric acid (1 M) by 2-(1H-benzo[d]imidazol-2-yl)-3-phenylacrylonitrile: gravimetric analysis and thermodynamic parameters

Guégué Jean Marie Vianney YOBO

Laboratoire de Réaction et Constitution de la Matière, Université Félix Houphouët BOIGNY, 22 BP 582 Abidjan 22, Côte d'Ivoire

Ahissan Donatien EHOUMAN*

Laboratoire de Thermodynamique et Physico-Chimie du Milieu, Université NANGUI ABROGOUA, 02 BP 801 Abidjan 02, Côte d'Ivoire
e-mail: ehoumandona@gmail.com

Kossitse Venyo AKPATAKU

Laboratoire de Chimie Organique et Sciences Environnementales, Faculté de Science et Technologie, Université de Kara, BP 404, Kara, Togo

Paulin Marius NIAMIEN

Laboratoire de Réaction et Constitution de la Matière, Université Félix Houphouët BOIGNY, 22 BP 582 Abidjan 22, Côte d'Ivoire

Abstract

This study evaluates the inhibitory effect of the organic compound 2-(1H-benzo[d]imidazol-2-yl)-3-phenylacrylonitrile on aluminum corrosion in a 1 M hydrochloric acid solution, using the mass loss method. The results show that the inhibitory efficiency increases with the concentration of the inhibitor, while it decreases as the temperature of the corrosive medium rises. To better understand the interactions between the metal surface and the inhibitor molecule, several adsorption isotherm models, notably those of Langmuir, Freundlich, Temkin, and El-Awady, were applied. The Dubinin–Radushkevich and Adejo–Ekwenchi isotherms helped clarify the mechanism and mode of inhibitor adsorption on aluminum. Furthermore, the thermodynamic parameters related to adsorption and activation phenomena were determined to explain the compound's inhibitory behavior in an acidic medium.

1. Introduction

The corrosion of aluminum in acidic media constitutes a major industrial problem despite the natural presence of a protective passive film on its surface [1]. Organic inhibitors, particularly benzimidazole derivatives, are widely studied due to their high adsorption capacity, which is attributed to the presence of heteroatoms and π-conjugated systems [2-3]. In this context, the molecule 2-(1H-benzo[d]imidazol-2-yl)-3-phenylacrylonitrile (BIPHA-4-H) appears to be a promising inhibitor due to the conjugation of the benzimidazole ring and the acrylonitrile group, which promotes its interaction with the metal surface and enhances its anticorrosive efficacy.

Received: April 18, 2026; Revised & Accepted: May 29, 2026; Published online: June 5, 2026

Keywords and phrases: aluminum, 2-(1H-benzo[d]imidazol-2-yl)-3-phenylacrylonitrile, gravimetric analysis, thermodynamic parameters.

*Corresponding author

2. Materials and Methods

2.1. Aluminum Specimens

The material used in these tests consists of a 99.6% pure aluminum rod with a density 2.7, mass (0.1325 g ± 0.0001), having a cylindrical shape with a height of 1 cm and a diameter of 0.25 cm. The molecule under study, 2-(1H-benzo[d]imidazol-2-yl)-3-phenylacrylonitrile (BIPHA-4-H), is a synthesized organic molecule with the molecular formula $C_{16}H_{11}N_3$ and a molecular weight of 245.10 g/mol. Its percentage composition is as follows: C: 78.35%, H: 4.52%, N: 17.13%. Its structure is shown in Figure 1.

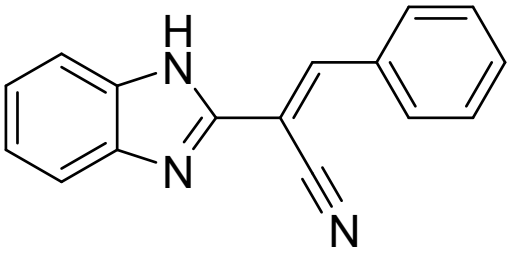

Figure 1. Structure of 2-(1H-benzo[d]imidazol-2-yl)-3-phénylacrylonitrile).

2.2. Prepared Solutions

A commercial solution (Sigma-Aldrich Chemicals) of hydrochloric acid with a purity of P = 37%, a density of d = 1.2, and a molar mass of M = 36.46 g/mol. A 1 M solution was prepared from this commercial solution. The prepared BIPHA-4-H solutions have concentrations of C = 0.005 mM, C = 0.01 mM, C = 0.05 mM, C = 0.1 mM, and C = 0.5 mM.

2.3. Mass Loss Method

Aluminum corrosion was evaluated using the gravimetric method (mass loss) [4–6]. The samples were immersed for 1 hour in 50 mL of hydrochloric acid solution, in the absence and in the presence of inhibitors, at temperatures ranging from 298 to 338 K in a thermostatic bath. The initial mass (m_1) and the final mass after immersion, cleaning, rinsing, and drying (m_2) were determined. The mass loss ($\Delta m = m_1 - m_2$) was calculated from the average of three tests conducted under the same conditions. The values obtained were used to determine the corrosion rate (W), the coverage ratio (θ), and the inhibition efficiency (EI %).

$$W = \frac{\Delta m}{St} \tag{1}$$

$$EI(\%) = \frac{W_0 - W}{W_0} \times 100 \tag{2}$$

$$\theta = \frac{W_0 - W}{W_0} \tag{3}$$

where W_0 and W are the corrosion rates in the absence and presence of the inhibitor, respectively; Δm is the mass loss, S is the total surface area of the aluminium sample, and t is the immersion time.

3. Results and Discussion

3.1. Corrosion Rate and Inhibitor Efficiency

Effect of temperature and inhibitor concentration on the corrosion rate

The corrosion rate of aluminum was studied in a molar solution of hydrochloric acid, first in the absence of

an inhibitor, then in the presence of organic inhibitors at various concentrations. The inhibitor BIPHA-4-H was evaluated at concentrations of 0.005 mM, 0.01 mM, 0.05 mM, 0.1 mM, and 0.5 mM, and over a temperature range from 298 to 338 K.

Figure 2 illustrates the influence of concentration and temperature on the corrosion rate of aluminum in the presence of the BIPHA-4-H inhibitor.

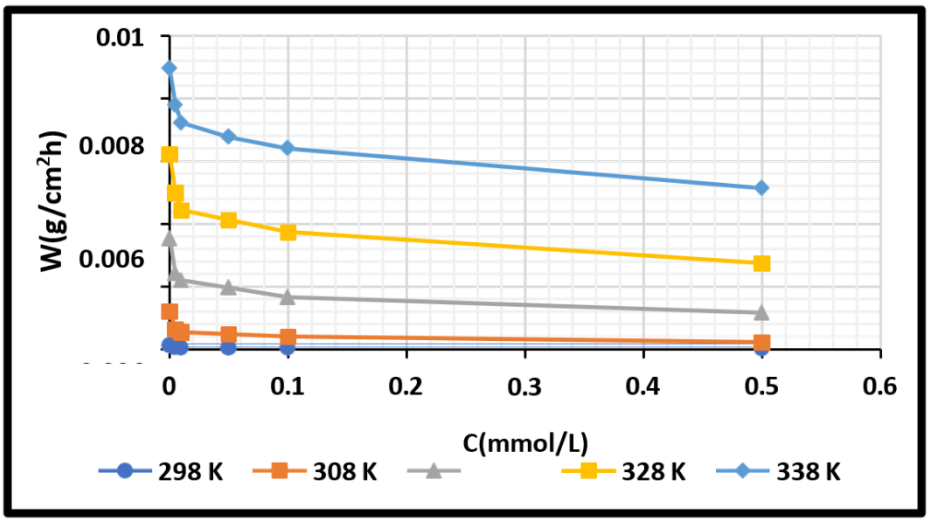

Figure 2. Corrosion rate as a function of BIPHA-4-H concentration at different temperatures.

The BIPHA-4-H molecule exhibits good inhibitory efficacy against aluminum corrosion in a 1 M HCl solution. The corrosion rate decreases as its concentration increases due to its adsorption onto the metal surface and the formation of a protective film [7]. However, elevated temperatures reduce this effectiveness by weakening the protective layer formed [8]. These results are consistent with those of Yeo et al. [9]. The inhibitory action of BIPHA-4-H is linked to the presence of nitrogen atoms, which promote its adsorption onto aluminum [10].

3.2. Influence of Temperature and Concentration on Inhibitory Efficacy

The variation in the inhibitory efficacy of BIPHA-4-H as a function of concentration at different temperatures is illustrated in Figure 3.

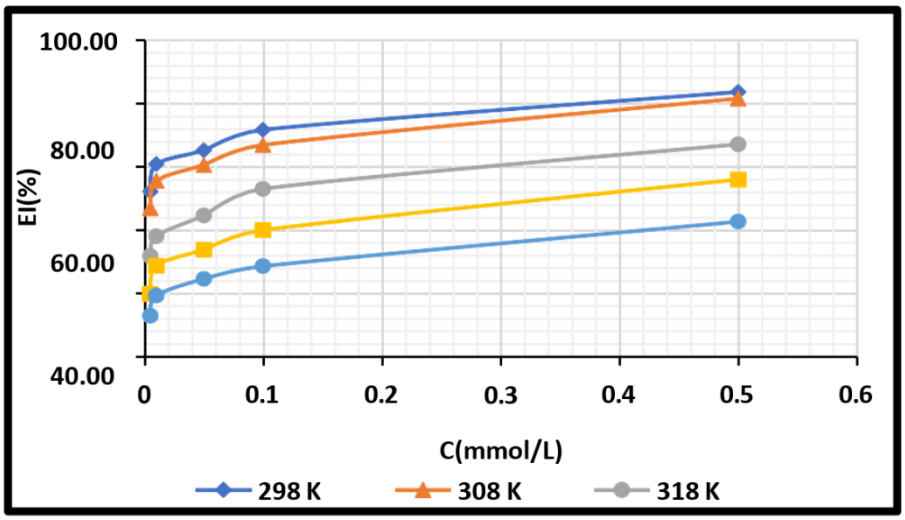

Figure 3. Changes in inhibitory activity as a function of BIPHA-4-H concentration at different temperatures.

The inhibitory efficacy of the BIPHA-4-H molecule decreases as the temperature rises due to the gradual degradation of the protective film adsorbed onto the aluminum surface [7]. This behavior reflects a primarily physical adsorption mechanism [10]. Conversely, the inhibitory efficiency increases with the concentration of BIPHA-4-H due to greater adsorption of the molecules onto the metal surface [11]. The highest efficiency obtained for BIPHA-4-H is 96.09% at 298 K.

3.3. Kinetic Aspect (Influence of Immersion Time)

To study the inhibitory efficacy of the inhibitory molecules over time, aluminum samples were immersed in 1 M hydrochloric acid solutions, with and without the addition of our molecule at a concentration of 0.5 mM, at a temperature of 298 K for immersion durations of 1 h, 2 h, 4 h, 6 h, and 19 h. Figure 4 shows the evolution of inhibition efficiency as a function of immersion time.

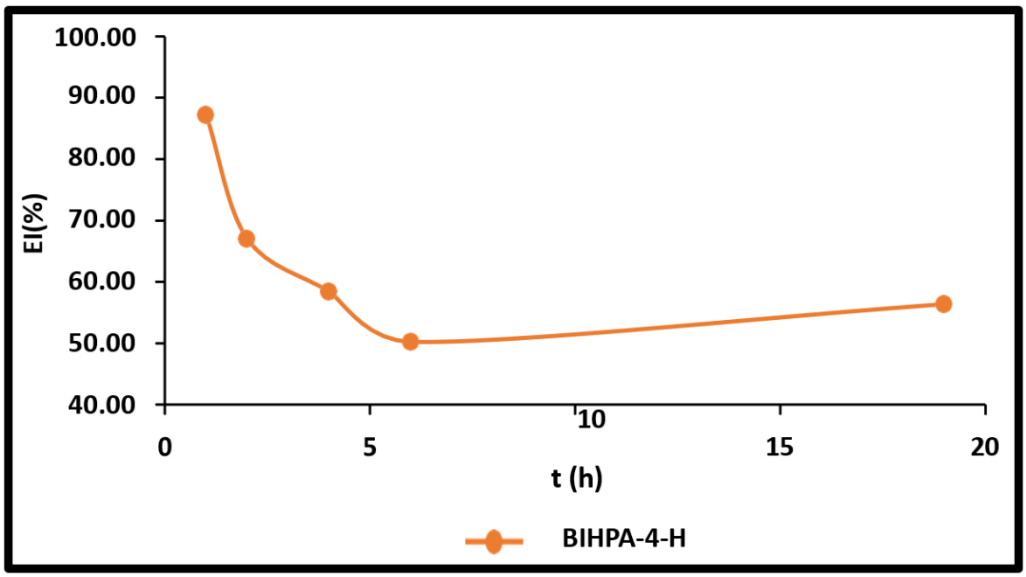

Figure 4. Changes in the inhibitory efficacy of BIPHA-4-H as a function of immersion time.

The inhibitory efficacy gradually decreases between 1 and 6 hours of immersion, then stabilizes up to 19 hours, consistent with the findings in [9]. This behavior reflects the initial formation of a protective film on the aluminum, followed by a slight desorption of the inhibitory molecules before the metal protection stabilizes.

3.4. UV-Visible Spectroscopy

UV-visible absorption spectroscopy provides additional information on the interactions between aluminum and the inhibitor in solution and may allow verification of layer formation on the metal surface. 1 M HCl solutions containing 0.5 mM BIPHA-4-H are analyzed before and after immersing the aluminum for 4 hours at 298 K. The results are presented in Figure 5.

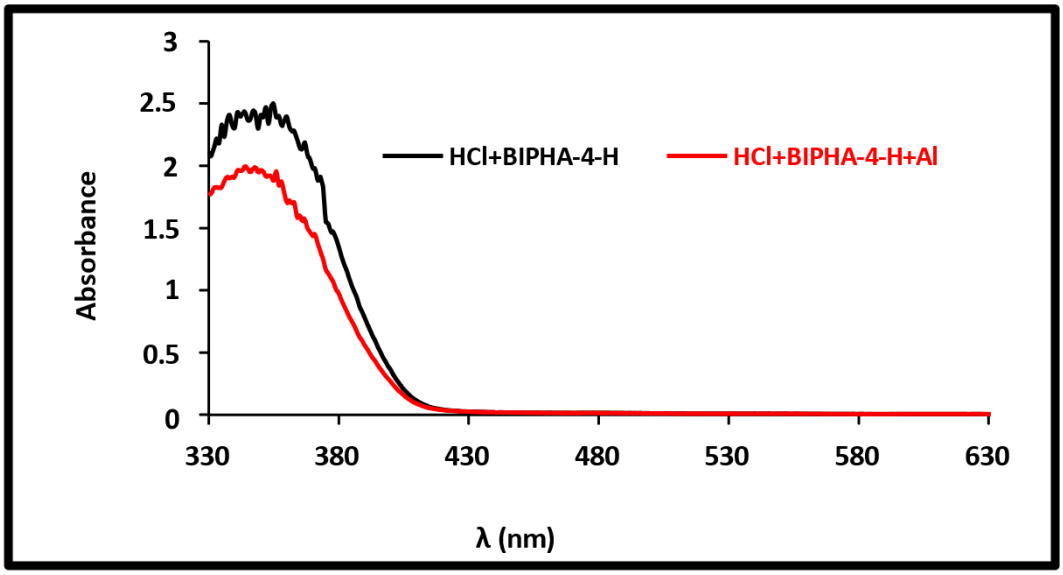

Figure 5. UV-Vis spectrum of a 1 M HCl solution containing 0.5 mM BIPHA-4-H before and after immersing the aluminum for 4 hours at 298 K.

Before immersion, the solution containing BIPHA-4-H exhibits a UV-visible absorption peak at 355 nm, characteristic of the n-π* transitions associated with the nitrogen atoms of the benzimidazole-acrylonitrile ring. After 4 hours of aluminum immersion, this peak shifts to 350 nm with a decrease in intensity, indicating the formation of a protective BIPHA-4-H film on the metal surface [12].

3.5. Adsorption Isotherms

Langmuir Isotherm

To study this model, we plotted the Cinh/θ curves as a function of Cinh for each inhibitor tested. The Cinh/θ curve as a function of Cinh is shown in Figure 6 for the BIPHA-4-H molecule.

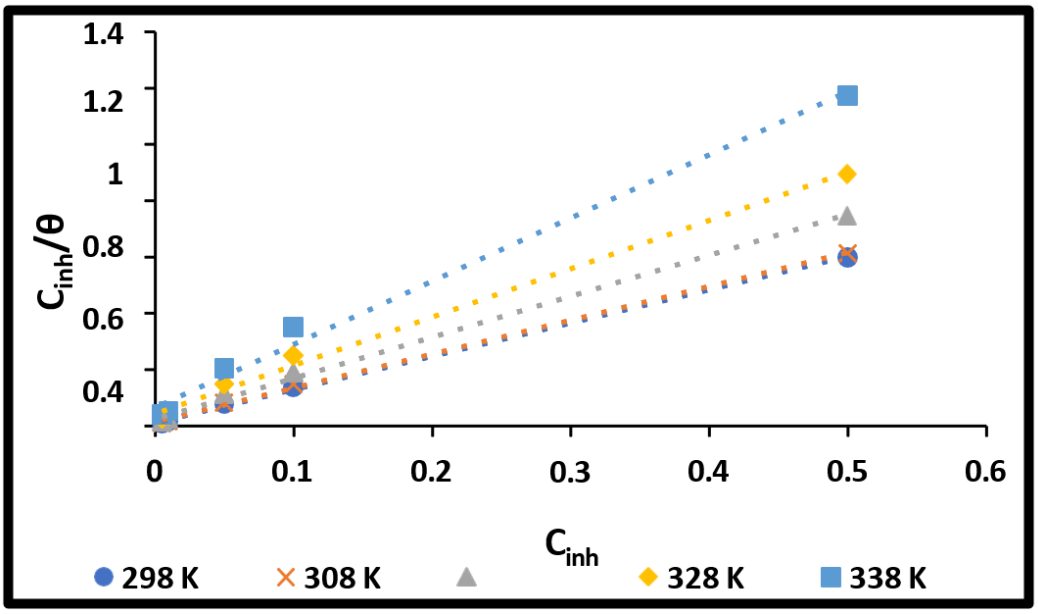

Figure 6. Plot of Cinh/θ versus Cinh for the BIPHA-4-H molecule.

Table 1. Langmuir model parameters for BIPHA-4-H molecules

Inhibitor	T(K)	Equation	R^2	$K_{ads}(M^{-1})$
BIPHA-4-H	298	$C_{inh}/\theta = 1.1772C_{inh} + 0.0113$	0.9989	104176.99
	308	$C_{inh}/\theta = 1.2026C_{inh} + 0.0147$	0.9982	81809.52
	318	$C_{inh}/\theta = 1.4497C_{inh} + 0.0246$	0.9972	58930.89
	328	$C_{inh}/\theta = 1.7190C_{inh} + 0.0414$	0.9942	41521.739
	338	$C_{inh}/\theta = 2.2392C_{inh} + 0.0650$	0.9918	34449.231

For the BIPHA-4-H molecule, the linear relationship obtained between Cinh/θ and Cinh, with a coefficient of determination R^2 close to unity, shows that its adsorption on the aluminum surface follows the Langmuir isotherm. This result indicates that BIPHA-4-H molecules occupy a single adsorption site on the metal surface in an HCl environment.

El-Awady Isotherm

The fit of the experimental data to the El-Awady model, where log(θ/1-θ) = f(log(Cinh)), is shown in Figure 7 for the BIPHA-4-H molecule.

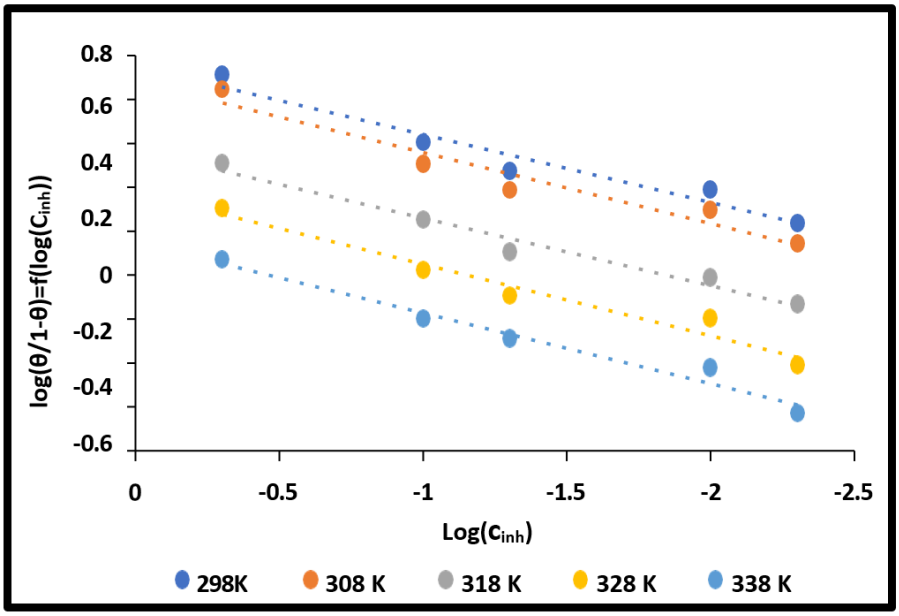

Figure 7. Plot of log(θ/(1-θ)) versus log(Cinh) for the BIPHA-4-H molecule.

The parameters of El-Awady's model for the molecule are listed in Table 2.

Table 2. Parameters of El-Awady's model for the BIPHA-4-H molecule

Inhibitor	T(K)	Equation	R^2	1/y
BIPHA-4-H	298	$\log(\theta/(\theta\text{-}1)) = 0.3097\log(C_{inh}) + 0.7511$	0.9481	3.2289
	308	$\log(\theta/(\theta\text{-}1)) = 0.3223\log(C_{inh}) + 0.6817$	0.943	3.1027
	318	$\log(\theta/(\theta\text{-}1)) = 0.3072\log(C_{inh}) + 0.3700$	0.9737	3.2552
	328	$\log(\theta/(\theta\text{-}1)) = 0.3248\log(C_{inh}) + 0.1757$	0.9601	3.0788
	338	$\log(\theta/(\theta\text{-}1)) = 0.3208\log(C_{inh}) - 0.0489$	0.9707	3.1172

For the BIPHA-4-H molecule, the results show a good correlation with the El-Awady model, with an R^2 coefficient close to unity, indicating a satisfactory fit for adsorption on aluminum in an HCl environment. However, the value of the 1/y parameter being greater than 1 suggests that the BIPHA-4-H molecule occupies multiple active sites during its adsorption onto the metal surface [13].

Temkin isotherm

The variation of the coverage (θ) as a function of log(Cinh) was plotted for the inhibitor at different temperatures. The curves obtained for the BIPHA-4-H molecules are presented in Figure 8.

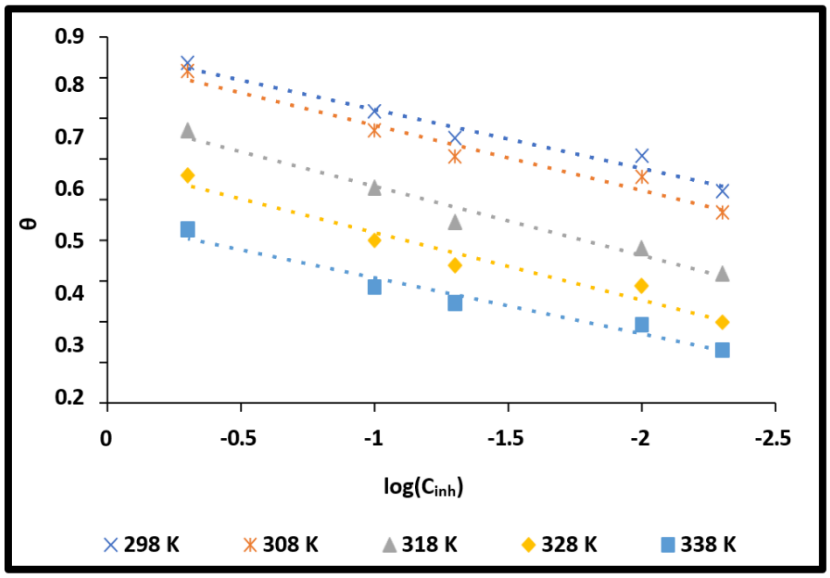

Figure 8. Variation in the recovery rate (θ) as a function of log (Cinh) for BIPHA-4-H.

Table 3. Parameters of the Temkin model for BIPHA-4-H molecules

Inhibitor	T(K)	Equation	R^2	a
BIPHA-4-H	298	$\theta = 0.1375\log(C_{inh}) + 0.4462$	0.9611	-8.37
	308	$\theta = 0.1605\log(C_{inh}) + 0.8448$	0.9623	-7.20
	318	$\theta = 0.1701\log(C_{inh}) + 0.7044$	0.9732	-6.77
	328	$\theta = 0.1665\log(C_{inh}) + 0.5867$	0.9571	-6.92
	338	$\theta = 0.1457\log(C_{inh}) + 0.8686$	0.9639	-7.90

For the BIPHA-4-H molecule, correlation coefficients close to unity indicate that the model accurately describes its adsorption on aluminum in an HCl environment. The negative values of the interaction constant reflect repulsive forces between the adsorbed molecules, which increase with temperature (298–318 K), explaining the decrease in the inhibitory efficacy of BIPHA-4-H at high temperatures.

3.6. Model and Type of Adsorption

Identification of the appropriate adsorption model

After analyzing the adsorption isotherms, it is necessary to determine which isotherm best describes the adsorption of the studied inhibitor molecules onto aluminum in a 1 M HCl medium. To do this, a comparison of the coefficients of determination must be performed to select the model that best reflects the adsorption of each

inhibitor onto the aluminum surface. Table 4 presents the correlation coefficients of the models studied for our inhibitor.

Table 4. Comparison of the correlation coefficients of the different models for each inhibitor.

Inhibitor	T(K)	Langmuir	Temkin	El awady
BIPHA-4-H	298	0.9989	0.9611	0.9481
	308	0.9982	0.9623	0.943
	318	0.9972	0.9732	0.9737
	328	0.9942	0.9571	0.9601
	338	0.9918	0.9639	0.9707

An analysis of Table 4 shows that the Langmuir model yields correlation coefficients closest to unity compared to the El-Awady and Temkin models, indicating that it best describes the adsorption of inhibitors on the aluminum surface. However, the slopes obtained (Table 5) are greater than one, suggesting that a single inhibitor molecule occupies multiple adsorption sites. This deviation could be related to repulsive interactions between species adsorbed on the metal surface. Thus, adsorption does not strictly follow the classical Langmuir isotherm, but is better described by the modified Langmuir isotherm, or Villamil model:

$$\frac{C_{inh}}{\theta} = \frac{n}{K_{ads}} + nC_{inh} \quad (4)$$

n is a constant introduced to account for all factors not taken into account in the derivation of the Langmuir isotherm.

Table 5. Slopes obtained for BIPHA-4-H inhibitors using the Langmuir model.

T°(k)	298	308	318	328	338
Slopes	1.1772	1.2026	1.4497	1.7190	2.2392

3.7. Determination of Thermodynamic Parameters Related to the Adsorption of BIPHA-4-H on Aluminum

The appropriate adsorption isotherm allows for the evaluation of the thermodynamic parameters of adsorption. The standard free energy of adsorption, ΔG°ads, was calculated using the following equation:

$$\Delta G^0_{ads} = -RTln(55{,}5K_{ads}) \quad (5)$$

where R is the ideal gas constant, T is the absolute temperature, and 55.5 is the concentration of water in mol.L^{-1}, the values of ΔG^0_{ads} obtained are listed in Table 6 below:

Table 6. Values of thermodynamic parameters related to the adsorption of BIPHA-4-H on aluminum

T(K)	K_{ads} (M^{-1})	ΔG^0_{ads} (kJ.mol^{-1})	ΔH^0_{ads} (kJ.mol^{-1})	ΔS^0_{ads} (J.mol^{-1}.K^{-1})
298	104176.99	-21.5	-24.226	48.3
308	81809.52	-29.23		
318	58930.89	-29.64		
328	41521.739	-39.93		
338	34449.231	-40.63		

We observe very high values of the adsorption constant across the entire temperature range, particularly at 298 K and 308 K. These high values indicate a very large number of BIPHA-4-H molecules adsorbed onto the metal surface, especially at 298 K and 308 K [14–15]. According to the literature, a value of ΔG^0_{ads} below -40 kJ.mol⁻¹ would indicate a chemical adsorption process (chemisorption), whereas a value above -20 kJ.mol⁻¹ would instead indicate a physical adsorption process (physisorption). For values between -40 kJ.mol⁻¹ and -20 kJ.mol⁻¹, both types of adsorption are believed to occur [16].

The changes in adsorption enthalpy ΔH^0_{ads} and entropy ΔS^0_{ads} are calculated using the following equation:

$$\Delta G^0_{ads} = \Delta H^0_{ads} - T\Delta S^0_{ads} \quad (6)$$

where $\Delta H^0_{ads}\ and\ \Delta S^0_{ads}$, respectively, they-intercept and the negative slope of the line obtained from the curve showing the variation of ΔG^0_{ads} as a function of temperature (Figure 9).

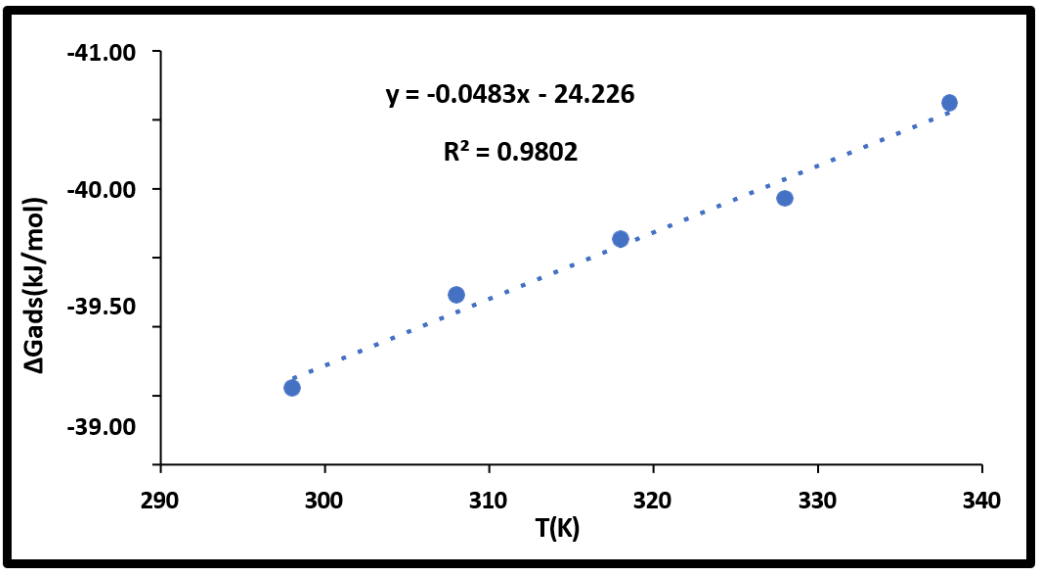

Figure 9. Variation of ΔG^0_{ads} a function of temperature.

The negative values of the free enthalpy of adsorption demonstrate the spontaneous nature of the adsorption process [15]. Figure 9 shows that the plot of ΔG^0_{ads} versus temperature is a straight line with a slope of ($-\Delta S^0_{ads}$) and a y-intercept of (ΔH^0_{ads}). From the equation of this line, we find that ΔH^0_{ads} = -24.226 kJ.mol^{-1} et ΔS^0_{ads} = 48.3 J.mol^{-1} K^{-1}. The negative sign of the change in adsorption enthalpy indicates an exothermic adsorption process, while the positive sign of the change in entropy shows that disorder increases during the adsorption phase, likely due to the desorption of water molecules [17]. However, since the values are closer to −20 kJ·mol⁻¹ than to −40 kJ·mol⁻¹, the adsorption process is predominantly governed by physisorption, with a minor contribution from chemisorption. Most ΔG°ads values range from −21.15 to −29.64 kJ·mol⁻¹, suggesting that the adsorption mechanism involves both physisorption and chemisorption.

3.8. Type of Adsorption

To interpret the adsorption mode of our molecule, we used the Adejo-Ekwenchi and Dubinin-Radushkevich isotherms, with the respective equations:

$$\log[1/(1-\theta)] = logK_{AE} + b\ logC \quad (7)$$

Where K_{AE} and are the parameters of the isotherm, and C is the concentration of the adsorbate.

$$ln\theta = ln\theta_{max} - a\delta^2 \quad (8)$$

$$\text{Avec :} \quad \delta = RTln\left(1 + \frac{1}{MC_{inh}}\right) \quad (9)$$

$E_{ads}^{m} = \frac{1}{\sqrt{2a}}$ (Average adsorption energy in kJ/mol)

To confirm the mechanism of inhibitor adsorption on the metal surface, the parameters of the Adejo-Ekwenchi isotherm were determined at different temperatures in the corrosive media studied. Figure 10 shows the variation of log[1/(1 − θ)] as a function of log Cinh. The values of the associated parameters are listed in Table 7 below:

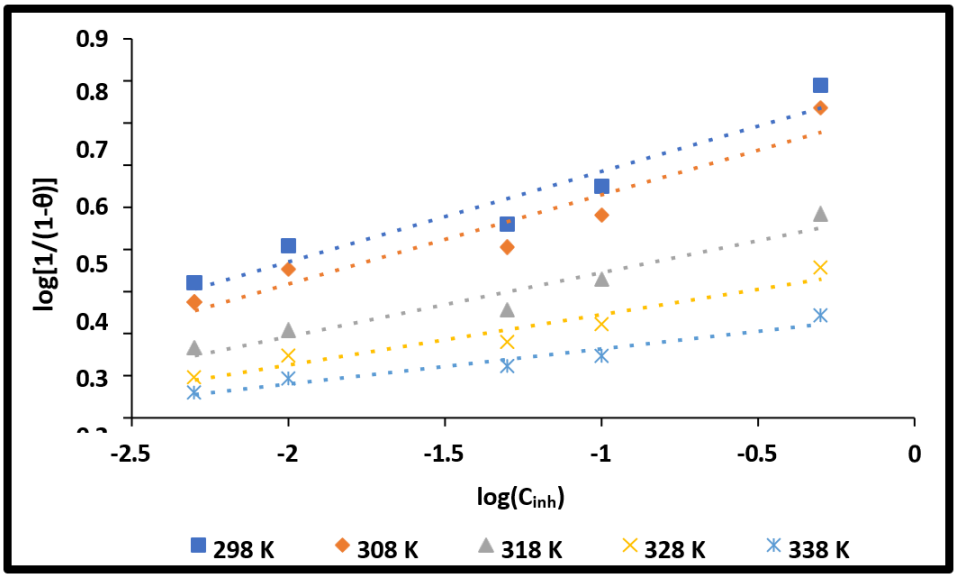

Figure 10. Adejo-Ekwenchi isotherm curves for BIPHA-4-H in HCl solution

Table 7 below presents the parameters of the Adejo-Ekwenchi adsorption isotherm.

Table 7. Parameters of the Adejo-Ekwenchi adsorption isotherm

Parameters Adejo-Ekwenchi					
T(K)	298	308	318	328	338
b	0.2153	0.2115	0.1512	0.1197	0.0837

This table also shows that the indicator parameter b does not remain relatively constant. This variation suggests that the adsorption of BIPHA-4-H molecules onto the aluminum surface in a hydrochloric acid environment is primarily physical in nature (with physisorption predominating) [18].

3.9. Activation Parameters of the Corrosion Process

The thermodynamic activation parameters (activation energy E_a, activation enthalpy change ΔH_a^* nd activation entropy change ΔS_a^*) for the corrosion process were determined using the Arrhenius and transition state equations [19].

$$logW = logA - \frac{E_a}{2.3RT} \quad (10)$$

$$log\left(\frac{W}{T}\right) = \left[log\left(\frac{R}{Nh}\right) + \frac{\Delta S_a^*}{2.303R}\right] - \frac{\Delta H_a^*}{2.303RT} \quad (11)$$

W is the corrosion rate, R is the ideal gas constant, A is the pre-exponential factor, h is Planck's constant, and א is Avogadro's constant, E_a is the activation energy, ΔH_a^*, is the activation enthalpy change and ΔS_a^* is the activation entropy change.

Figure 11 shows the Arrhenius curves of log W versus 1/T for aluminum in a 1 M HCl solution with and without different concentrations of our inhibitor. The straight lines were obtained with correlation coefficients ($R^2 > 0.9$). The slopes ($-\frac{E_a}{2,3RT}$) of these lines are used to calculate the apparent activation energy (E_a). The values of the thermodynamic activation parameters are given in Table 8.

Table 8. Thermodynamic parameters for the dissolution of aluminum in 1 M HCl with and without different concentrations of the BIPHA-4-H inhibitor

Concentration (mM)	$E_a(kJ.mol^{-1})$	$\Delta H_a^*(kJ.mol^{-1})$	$\Delta S_a^*(J.mol^{-1}.K^{-1})$
Blank	86.80	-84.16	-31.99
0.005	100.29	97.65	7.00
0.01	102.91	100.27	14.14
0.05	104.13	101.49	17.17
0.1	107.31	104.67	26.01
0.5	115.12	112.48	47.27

Figure 11 below shows log (W/T) versus 1/T

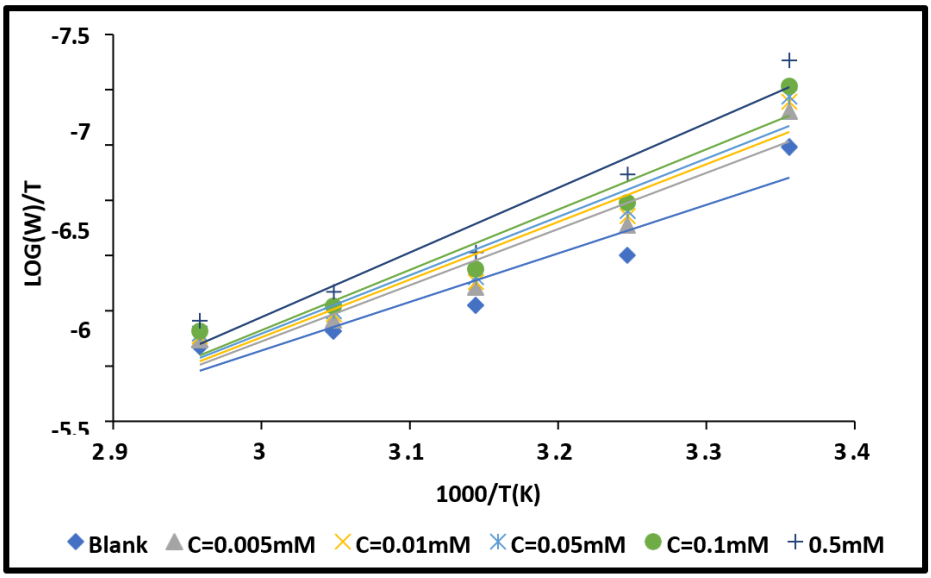

Figure 11. Variation of log W as a function of 1/T for different concentrations.

Analysis of Table 8 above reveals that the activation enthalpy (ΔHa) values are positive and increase across the entire concentration range studied, indicating that the aluminum dissolution process remains endothermic in the presence of the inhibitor. Furthermore, the activation entropy (ΔSa) generally tends to increase with the concentration of BIPHA-4-H, although negative values are observed at 298 K and 338 K, reflecting a decrease in the order of the system during the formation of the activated state [20].

Conclusion

The compound BIPHA-4-H has been shown to be an effective inhibitor of aluminum corrosion in 1 M HCl solution. Its inhibitory effectiveness increases with the inhibitor concentration and varies with temperature. The study of adsorption isotherms showed that the adsorption of BIPHA-4-H onto the aluminum surface follows the modified Langmuir model, indicating the formation of an adsorbed protective layer. The calculated thermodynamic parameters of adsorption and activation suggest that the inhibition mechanism is dominated by physisorption, involving electrostatic interactions between the inhibitor molecules and the metallic surface. These results confirm the potential of BIPHA-4-H as a promising inhibitor for the protection of aluminum in acidic environments.

References

[1] Mu, G., Li, X., Qu, Q., & Zhou, J. (2006). Molybdate and tungstate as corrosion inhibitors for cold rolling steel in hydrochloric acid solution. *Corrosion Science*, *48*(2), 445–459. https://doi.org/10.1016/j.corsci.2005.01.013

[2] Abdallah, M., Fawzy, A., & Al Bahir, A. (2020). The effect of expired acyclovir and omeprazole drugs on the inhibition of Sabic iron corrosion in HCl solution. *International Journal of Electrochemical Science*, *15*(5), 4739–4753. https://doi.org/10.20964/2020.05.86

[3] Abdel Nazeer, A., El-Abbasy, H. M., & Fouda, A. S. (2013). Antibacterial drugs as environmentally-friendly corrosion inhibitors for carbon steel in acid medium. *Research on Chemical Intermediates, 39*, 921–939. https://doi.org/10.1007/s11164-012-0605-y

[4] Abu Orabi, F. M., Abu-Orabi, S. T., Fodeh, O. A., Algethami, F. K., Rawashdeh, A. M. M., Bataineh, T. T., Al-Mazaideh, G. M., & Al-Qudah, M. A. (2024). *Ajuga orientalis* L. extract as a green corrosion inhibitor of aluminum in an acidic solution: an experimental and DFT study. *Metals*, *14*(11), 1227. https://doi.org/10.3390/met14111227

[5] Musa, A. Y., Khadom, A. A., Kadhum, A. A. H., Mohamad, A. B., & Takriff, M. S. (2010). Kinetic behavior of mild steel corrosion inhibition by 4-amino-5-phenyl-4H-1,2,4-triazole-3-thiol. *Journal of the Taiwan Institute of Chemical Engineers*, *41*(1), 126–128. https://doi.org/10.1016/j.jtice.2009.08.002

[6] Rahim, A. A., & Kassim, J. (2008). Recent development of vegetal tannins in corrosion protection of iron and steel. *Recent Patents on Materials Science*, *1*(3), 223–231. https://doi.org/10.2174/1874464810801030223

[7] Sehmi, A., Ouici, H. B., Guendouzi, A., Ferhat, M., Benali, O., & Boudjellal, F. (2020). Corrosion inhibition of mild steel by newly synthesized pyrazole carboxamide derivatives in HCl acid medium: Experimental and theoretical studies. *Journal of The Electrochemical Society*, *167*(15), 155508. https://doi.org/10.1149/1945-7111/abab25

[8] Rhb, B. (2019). Theobromine as an aluminium corrosion inhibitor in 1 M HCl: Experimental and QSPR studies. *Journal of Chemical and Pharmaceutical Research*, *11*(12), 73–91.

[9] Yeo, M., Tigori, M. A., Kouyaté, A., Niamien, P. M., & Trokourey, A. (2020). Inhibition of aluminium corrosion in 1 M HCl by pyridoxine hydrochloride: Thermodynamic and quantum chemical studies. *International Research Journal of Pure and Applied Chemistry*, *21*(21), 20–38. https://doi.org/10.9734/irjpac/2020/v21i2130286

[10] Verma, C., Lgaz, H., Verma, D. K., Ebenso, E. E., Bahadur, I., & Quraishi, M. A. (2018). Molecular dynamics and Monte Carlo simulations as powerful tools for study of interfacial adsorption behavior of corrosion inhibitors in aqueous phase: A review. *Journal of Molecular Liquids*, *260*, 99–120. https://doi.org/10.1016/j.molliq.2018.03.045

[11] Touré, H. R., Bamba, A., Ehouman, A. D., Yeo, M., Tigori, M. A., & Trokourey, A. (2024). Study of the inhibitory properties of 2-((benzylthio)methyl)-1H-benzo[d]imidazole with respect to the corrosion of aluminum in a nitric acid medium. *Earthline Journal of Chemical Sciences*, *11*(3), 471–487. https://doi.org/10.34198/ejcs.11324.471487

[12] Oubahou, M., Rbaa, M., Lgaz, H., Takky, D., Naimi, Y., Alrashdi, A. A., & Lee, H. S. (2024). Exploring sustainable corrosion inhibition of copper in saline environment: An examination of hydroquinazolinones via experimental and ab initio DFT simulations. *Arabian Journal of Chemistry*, *17*(5), 105716. https://doi.org/10.1016/j.arabjc.2024.105716

[13] Adamu, A. A., Iyun, O. R. A., & Habila, J. D. (2025). Adsorption and thermodynamic studies of the corrosion inhibition effect of *Desmodium adscendens* (Swartz) extract on carbon steel in 2 M HCl. *BMC Chemistry*, *19*(1), 1–10. https://doi.org/10.1186/s13065-025-01541-y

[14] Fiala, A., & Mechehoud, Y. (2012). Étude de l'effet inhibiteur du 2-(1,3-dithiétan-2-ylidène)-3-oxobutanoate de méthyle et du 2-(1,3-dithiolane-2-ylidène)-3-oxobutanoate de méthyle sur la corrosion du cuivre en milieu nitrique 3 mol·L^{-1}. *Sciences & Technologie, Section A*, *35*, 23–30.

[15] Bockris, J. O'M., & Reddy, A. K. N. (1977). *Modern Electrochemistry* (Vol. 2). New York: Plenum Press. https://doi.org/10.1007/978-1-4615-7452-1

[16] Timoudan, N., Al-Gorair, A. S., El Foujji, L., Warad, I., Safi, Z., Dikici, B., Benhiba, F., El Kacem Qaiss, A., Bouhfid, R., Bentiss, F., Al-Juaid, S. S., Abdallah, M., & Zarrouk, A. (2024). *Corrosion inhibition performance of benzimidazole derivatives for protection of carbon steel in hydrochloric acid solution*. *RSC Advances*, *14*(41), 30295–30316. https://doi.org/10.1039/D4RA05070C

[17] Banerjee, G., & Malhotra, S. N. (1992). Adsorption behavior of corrosion inhibitors on metal surfaces. *Corrosion Science*, *32*(10), 1051–1060.

[18] Adejo, S. O., Ekwenchi, M. M., Gbertyo, J. A., Menengea, T., & Ogbodo, J. O. (2014). Determination of adsorption isotherm model best fit for methanol leaf extract of *Securinega virosa* as corrosion inhibitor for mild steel in HCl. *Journal of Advances in Chemistry*, *10*(5), 2737–2742. https://doi.org/10.24297/jac.v10i5.891

[19] Al-Amiery, A. A., Isahak, W. N. R. W., & Al-Azzawi, W. K. (2023). Corrosion inhibitors: Natural and synthetic organic inhibitors. *Lubricants*, *11*(4), 174. https://doi.org/10.3390/lubricants11040174

[20] Aphouet, A. K., N'Guadi, B. A., Mougo, A. T., Teminfolo, Y. S., Trokourey, A., & Niamien, P. M. (2023). Study of expired Fuclo 500 drug as an environmentally sustainable corrosion inhibitor. *European Journal of Chemistry*, *14*(3), 353–361. https://doi.org/10.5155/eurjchem.14.3.353-361.2443